

## Electronic Supplementary Information

### **3D origami multiplex electrochemical immunodevice based on nanoporous silver-paper electrode and metal ion functionalized nanoporous gold-chitosan**

Weiping Li,<sup>a</sup> Long Li,<sup>b</sup> Meng Li,<sup>a</sup> Jinghua Yu,<sup>a</sup> Shenguang Ge,<sup>b</sup> Mei Yan\*<sup>a</sup> and Xianrang Song\*<sup>c</sup>

<sup>a</sup> Key Laboratory of Chemical Sensing & Analysis in Universities of Shandong, School of Chemistry and Chemical Engineering, University of Jinan, Jinan 250022 (P. R. China)

<sup>b</sup> Shandong Provincial Key Laboratory of Preparation and Measurement of Building Materials, School of Material Science and Engineering, University of Jinan, Jinan 250022 (P.R. China)

<sup>c</sup> Cancer Research Center, Shandong Tumor Hospital, Jinan 250117 (P.R. China)

\* Corresponding to: E-mail address: [ujn.yujh@gmail.com](mailto:ujn.yujh@gmail.com)

Tel: +86-531-82767161

Fax: +86-531-82765956

## Reagents

Antigens (carcinoembryonic antigen (CEA) and  $\alpha$ -fetoprotein (AFP)), mouse monoclonal capture antibodies (McAb<sub>1</sub>) and signal antibodies (McAb<sub>2</sub>) of two antigens were purchased from Linc-Bio Science Co. Ltd. (Shanghai, China). The clinical serum samples were from Shandong Tumor Hospital. Chitosan, bovine serum albumin (BSA), AgNO<sub>3</sub>, ascorbic acid (AA), poly-(allylamine hydrochloride) (PAH) and Tween-20 were obtained from Sigma-Aldrich Chemical Co. (USA). Glutaraldehyde (GA) was obtained from Shanghai Reagent Company (Shanghai, China). 20 mM AgNO<sub>3</sub> solution and 200 mM AA solution were prepared daily for silver-growth enhancement. Ultrapure water obtained from a Millipore water purification system (>18.2 M $\Omega$ , Milli-Q, Millipore) was used in all assays and solutions. Phosphate buffered solution (PBS) (pH 7.4, 10.0 mM) was prepared with NaH<sub>2</sub>PO<sub>4</sub> and Na<sub>2</sub>HPO<sub>4</sub>. The washing buffer was PBS (10.0 mM) containing 0.05% (w/v) Tween-20. PBS (10.0 mM) containing 0.5% (w/v) BSA and 0.5% (w/v) casein was used as blocking solution. HAc/NaAc solutions with different pH values were prepared by mixing the stock solutions of HAc and NaAc. All other reagents were of analytical grade and used as received. The Au/Ag alloy (42:58 wt%, 25  $\mu$ m thick) foils were obtained from Changshu Noble Metal Company. Carbon ink (ED423ss) and Ag/AgCl ink (CNC-01) were purchased from Acheson. Whatman chromatography paper #1 (58.0 cm  $\times$  68.0 cm) (pure cellulose paper) was obtained from GE Healthcare Worldwide (Pudong, Shanghai, China) and used with further adjustment of size (A4 size).

## Abbreviations

|             |   |
|-------------|---|
| EC          | electrochemical   |
| $\mu$ -PADs | microfluidic paper-based analytical devices                 |
| $\mu$ -OMEI | microfluidic origami multiplex electrochemical immunodevice |

|                    |                                  |
|--------------------|----------------------------------|
| PWE                | paper working electrode          |
| NPS                | nanoporous silver                |
| NGC                | nanoporous gold-chitosan         |
| PAH                | poly-(allylamine hydrochloride)  |
| GA                 | glutaraldehyde                   |
| AA                 | ascorbic acid                    |
| BSA                | bovine serum albumin             |
| PBS                | phosphate buffered solution      |
| SEM                | scanning electron microscopy     |
| TEM                | transmission electron microscopy |
| XPS                | X-ray photoelectron spectroscopy |
| SWV                | square wave voltammetry          |
| CEA                | carcinoembryonic antigen         |
| AFP                | r-fetoprotein                    |
| McAb <sub>1s</sub> | capture antibodies               |
| McAb <sub>2s</sub> | signal antibodies                |

### **Fabrication and characterization of this 3D origami EC device**

This 3D origami EC device was fabricated on pure cellulose paper within 10 min, and a detailed procedure was described below. Wax printing is rapid, inexpensive, and particularly well-suited for producing large lots (hundreds to thousands) of prototype  $\mu$ -PADs.<sup>1</sup> As shown in Scheme 1A, the entire paper-based device is 25.0 mm  $\times$  20.0 mm. The shape for hydrophobic barrier on origami EC device was designed using Adobe illustrator CS4. The entire origami device could be produced in bulk on an A4 paper sheet by a commercially available solid-wax printer (Xerox Phaser 8560N color printer) (Fig. S1A). Owing to the 3D porous structure of paper, the melted wax could penetrate into the paper to decrease the hydrophilicity of paper remarkably (Fig. S1B). For the wax-patterned paper, the printed area sustained an apparent contact angle for water

of 116° after the curing process, and the unprinted area maintained good flexibility, hydrophilicity and 3D porous structure would not affect the further screen-printing of electrodes and modifications.<sup>1,2</sup>

The unprinted hydrophilic area, which constituted the reservoir of the paper electrochemical cell, contains one paper auxiliary zone (8 mm in diameter) on auxiliary pad and one paper working zone (6 mm in diameter) on sample tab. The wax-penetrated paper sheet was then ready for screen-printing of electrodes on their corresponding paper zones (Scheme 1B). The electrode array consisted of a screen-printed Ag/AgCl reference electrode and carbon counter electrode on the paper auxiliary zone (Fig. S1C) and a screen-printed carbon working electrode (5 mm in diameter) on the paper working zone (Fig. S1D) respectively. Between the sample tab and auxiliary pad, the unprinted line (1 mm in width) was defined as fold line, which could ensure that the paper sample zone on the sample tab was properly and exactly aligned to the paper auxiliary zone on auxiliary pad after folding, due to the difference of flexibility between the printed and unprinted area after baking. Finally, the paper sheet was cut into individual origami device for further modifications (Scheme 1C). After folding, the three screen-printed electrodes (working electrode, reference electrode, and counter electrode) would be connected once the paper electrochemical cell was filled with solution (Scheme 1D).

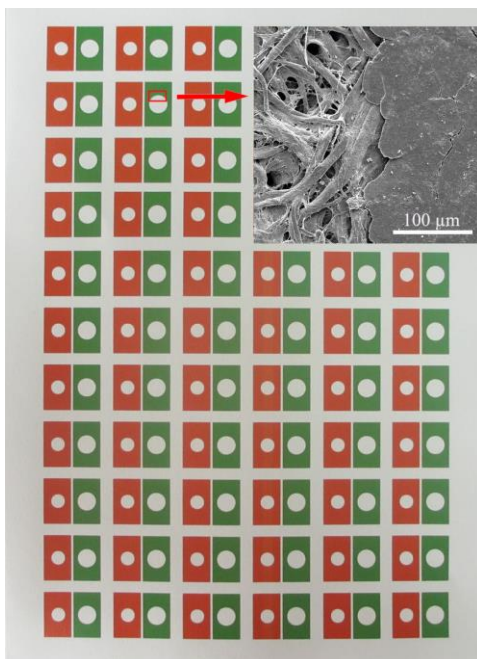


**Fig. S1A** Wax-printed 3D origami EC device on a paper sheet (A4) before baking. Inset: SEM image of the boundary of the wax-pattern: pure cellulose paper (left) and wax-printed paper (right).

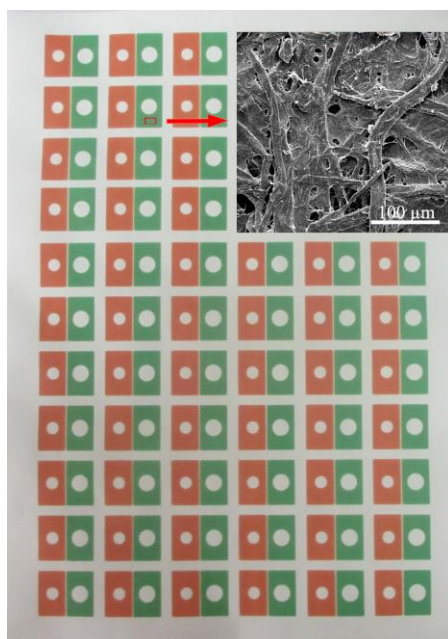


**Fig. S1B** Wax-printed 3D origami EC device on a paper sheet (A4) after baking. Inset: SEM image of the wax-penetrated cellulose paper.

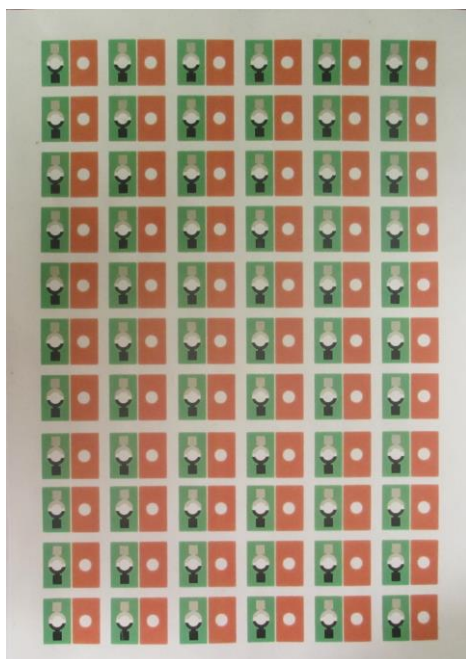


**Fig. S1C** 3D origami EC device on a paper sheet (A4) after screen-printing of Ag/AgCl auxiliary electrode and carbon counter electrode on one surface of paper.

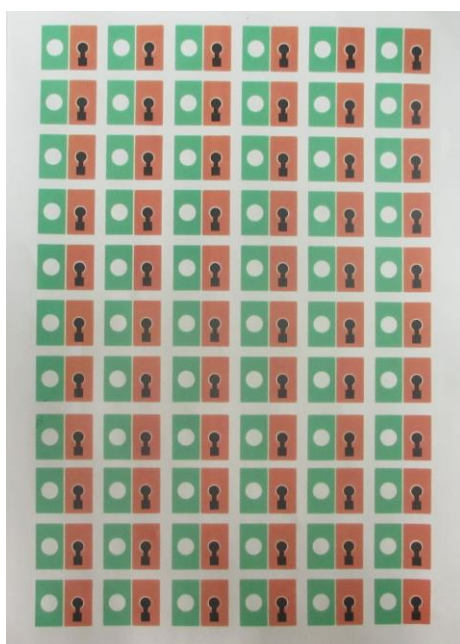


**Fig. S1D** 3D origami EC device on a paper sheet (A4) after screen-printing of carbon working electrode on one surface of paper.

### **Fabrication of NPS-PWE**

Prior to the immobilization, growth of NPS layer on the surfaces of cellulose fibers in the

paper working zone of PWE was implemented to fabricate novel NPS-PWE with enlarged effective surface area and enhanced conductivity for sensitive immunosensing. This novel NPS-PWE was fabricated on this 3D origami EC device through a direct chemical reduction of  $\text{AgNO}_3$  by AA. Briefly, 15  $\mu\text{L}$  of 20 mM  $\text{AgNO}_3$  solution was applied to one paper working zone on the back of a screen-printed carbon working electrode, followed immediately by the addition of 15  $\mu\text{L}$  of 200 mM AA solution, and incubated at room temperature for 10 min. Subsequently, the resulting NPS-PWE was washed with water thoroughly according to the method in our previous work.<sup>3</sup> Thus a layer of interconnected NPS on cellulose fibers with good conductivity was obtained (Scheme 2B), which was dried at room temperature for 20 min.

### **Characterizations of NPS-PWE**

The PWE was modified through the growth of an interconnected NPS layer on the surfaces of cellulose fibers in paper sample zone to fabricate this novel NPS-PWE. As shown in Fig. S3A, the bare paper sample zone, possessed high ratio of surface area to weight ( $9.5 \text{ m}^2/\text{g}$ )<sup>4</sup> with rough cellulose fibers, could offer an excellent adsorption microenvironment for silver nanoparticles. As the growth time increased (from 0 to 5 min), the silver nanoparticles were rapidly enlarged by incubating in the growth solution (Fig. S2A,B,C). Finally, as shown in Fig. S2D,E,F, a continuous and dense NPS conducting layer on the cellulose fiber surfaces in paper sample zone was observed, indicated that a good coverage of NPS on the surfaces of the cellulose fibers was obtained after 10 min of growth. The NPS modified paper sample zone maintained good porous structure after the growth process, which would benefit the further antibodies modification and analytical application. In addition, the successful immobilization of NPS on cellulose fibers was confirmed by XPS and the peaks observed at 368.2 and 374.2 eV were ascribed to metallic silver

(Fig. S3B).

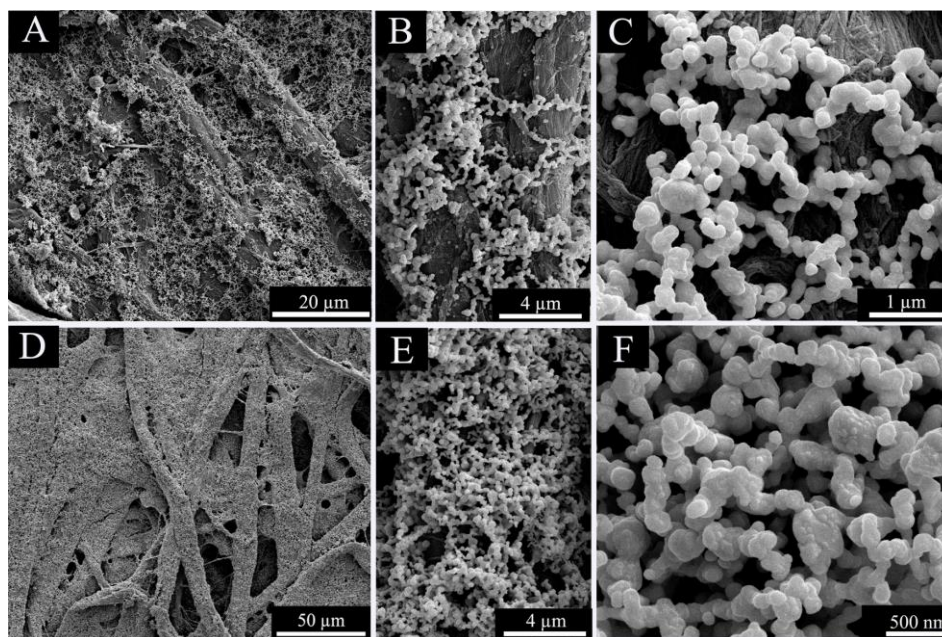


**Fig. S2** Growth of NPS layer on the surfaces of cellulose fibers in paper sample zone of PWE at different growth time under different magnification: A,B,C) After 5 min of growth; D,E,F) after 10 min of growth.

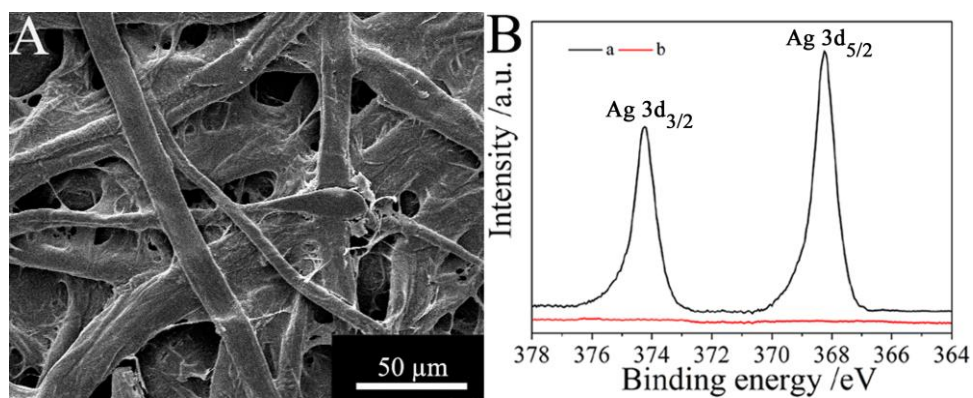


**Fig. S3** A) SEM image of bare paper sample zone of PWE; B) XPS of (a) NPS modified paper sample zone and (b) bare paper sample zone of PWE.

### Electrical resistivity of nanoporous silver modified paper sample zone

To measure the resistivity of NPS modified paper sample zone exactly, rectangular paper zones (1.0 mm×20.0 mm) were fabricated by wax-printing and then were modified through the growth of continuous and dense NPS conducting layer on the surfaces of cellulose fibers in these

rectangular paper zones using the same method described in experimental section under the same experimental conditions in each case, the average electrical resistivity of which revealed the electrical resistivity of NPS modified paper sample zone in this work. Prior to the measurements, both the bare and NPS modified rectangular paper zones were dried in a drying oven for 3 h. Then the measurements were performed with a four-point measurement setup using a digital multi-meter (Agilent, U1251B).

### **Preparation of McAb<sub>2</sub>/NGC-metal ion bioconjugates**

Nanoporous gold is made by selective dissolution (dealloying) of silver from silver/gold alloy according to the reported method.<sup>5</sup> Dealloying was carried out in 1:1 concentrated nitric acid at a constant temperature (25°C) for 10-15 min. The prepared nanoporous gold samples were washed to neutral with Milli-Q water. The obtained nanoporous gold was dispersed into chitosan solution (0.5 mg·mL<sup>-1</sup>) using sonication for 15 min to give a homogeneous solution.

For absorption of metal ion, 1 mL of nanoporous gold-chitosan (NGC) solution was dispersed in 10 mL of 10 mM Cu(NO<sub>3</sub>)<sub>2</sub> and Pb(NO<sub>3</sub>)<sub>2</sub> aqueous solution, respectively, and stirred for 24 h to reach equilibrium at room temperature. The pH of the solution was adjusted with 1 mol·L<sup>-1</sup> HCl solution. The NGC-metal ion were obtained by centrifugation and rinsed with water for several times. The resulted tracers were dispersed in 2 mL of Milli-Q water to get a dispersion of NGC-Cu<sup>2+</sup> and NGC-Pb<sup>2+</sup>. Next, 1 mL of the NGC-metal ion were dispersed in 1 mL of PAH (2 mg·mL<sup>-1</sup>) aqueous solution and sonicated for 20 min. Then, the tracers were washed with Milli-Q water and dispersed in 1 mL of GA (wt. 2.5%) and sonicated for 5 min. After washing with Milli-Q water and PBS for three times, 100 µL of anti-CEA McAb<sub>2</sub> (1 mg·mL<sup>-1</sup>) solution was added into the NGC-Cu<sup>2+</sup> and 100 µL of anti-AFP McAb<sub>2</sub> (1 mg·mL<sup>-1</sup>) solution was added into

the NGC-Pb<sup>2+</sup>, respectively, and shaken for 6 h. After centrifugation, the obtained bioconjugates were further washed with PBS for at least three times and resuspended in 4 mL of PBS as the assay solution.

### **Characterization of McAb<sub>2</sub>/NGC-metal ion bioconjugates**

The SEM image of the nanoporous gold displayed a type of sponge-like morphology with a 15-20 nm sized pore structure (Fig. S4A), which was further confirmed by TEM (inset, Fig. S4A). After chitosan was coated on the nanoporous gold, a smooth and uniform structure was observed (Fig. S4B), indicating the attachment of chitosan on nanoporous gold film through electrostatic adsorption. After the absorption of Cu<sup>2+</sup> and Pb<sup>2+</sup>, the morphologies of NGC-metal ion tracers did not change (Fig. S4C,D). In addition, elemental compositions of NGC-Cu<sup>2+</sup> and NGC-Pb<sup>2+</sup> tracers were analyzed with EDS (inset, Fig. S4C,D). Signature peaks of C, N, and O were observed for NGC hybrids. Meanwhile, the presence of Cu<sup>2+</sup> and Pb<sup>2+</sup> in the NGC-metal ion tracers was confirmed. Due to the incorporation of a large amount of metal ions (Cu<sup>2+</sup> and Pb<sup>2+</sup>), the NGC-metal ion tracers could be further used as labels in bioassay. McAb<sub>2</sub>s were obviously trapped on the surface of NGC-Cu<sup>2+</sup> and NGC-Pb<sup>2+</sup> tracers, indicating the successful fabrication of McAb<sub>2</sub>/NGC-metal ion tracers, which were shown in Fig. S4E,F.

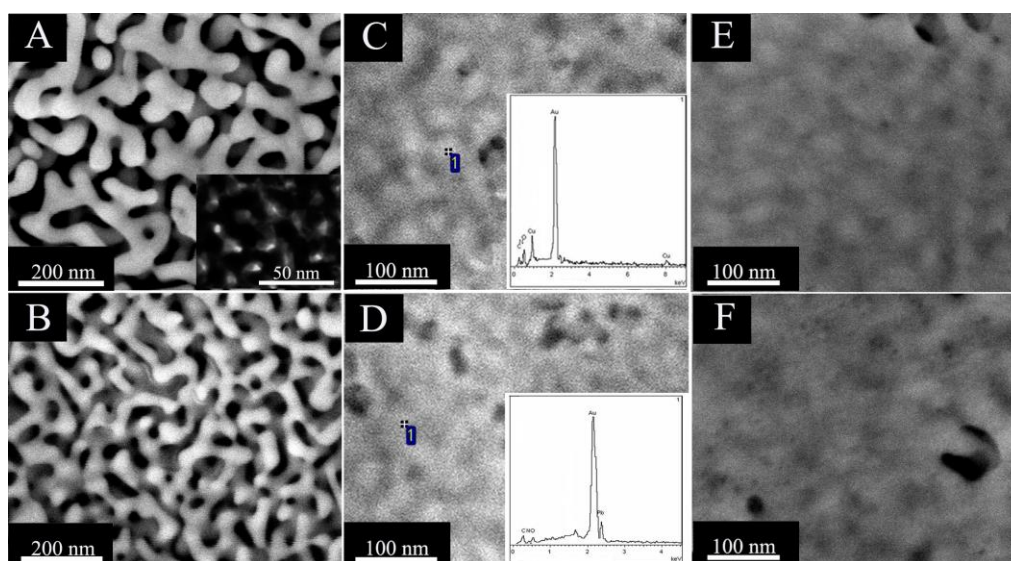


**Fig. S4** SEM images of A) nanoporous gold (inset, TEM image of nanoporous gold); B) NGC hybrid; C) NGC-Cu<sup>2+</sup> tracer (inset, EDS of NGC-Cu<sup>2+</sup> tracer); D) NGC-Pb<sup>2+</sup> tracer (inset, EDS of NGC-Pb<sup>2+</sup> tracer); E) anti-CEA McAb<sub>2</sub>/NGC-Cu<sup>2+</sup> tracer; F) anti-AFP McAb<sub>2</sub>/NGC-Pb<sup>2+</sup> tracer.

### Preparation of this $\mu$ -OMEI

As shown in Scheme 2, the  $\mu$ -OMEI was constructed by immobilizing McAb<sub>1</sub>s in one paper working zone of NPS-PWE. In brief, the mixture of McAb<sub>1</sub>s (4.0  $\mu$ L, 20.0  $\mu$ g·mL<sup>-1</sup>) was applied to the NPS-PWE, and incubated for 40 min. Subsequently, physically absorbed excess McAb<sub>1</sub>s were washed out with washing buffer. A drop of 4.0  $\mu$ L of blocking solution was then applied to the NPS-PWE and incubated for 40 min at room temperature to block possible remaining active sites against nonspecific adsorption. After another washing with washing buffer, the resulting  $\mu$ -OMEI was obtained and stored at 4 °C in a dry environment prior to use.

### EC assay procedure of this $\mu$ -OMEI

The electrochemical assay procedures of this  $\mu$ -OMEI were shown in Scheme 2, and a detailed procedure was described below. To carry out the immunoreaction and electrochemical measurement, the  $\mu$ -OMEI was firstly incubated with a 4.0  $\mu$ L of sample solution with different

concentrations of CEA and AFP in PBS for 160 s at room temperature, followed by washing with washing buffer. Next, the  $\mu$ -OMEI was further incubated with 4.0  $\mu$ L mixture of the designed tracers for 160 s at room temperature, followed by washing with washing buffer.

Finally, as shown in Scheme 1D, one sample tab was folded down below the auxiliary pad successively and clamped into the device-holder, which was comprised of two circuit boards (named Board-A and Board-B respectively below) with conductive pads on them, to fix and connect this  $\mu$ -OMEI to the electrochemical workstation. The electrochemical measurements were carried out in 50  $\mu$ L of HAc/NaAc (0.1 M) at pH 4.5. A SWV scan from  $-0.6$  V to 0 V with a pulse amplitude of 25 mV, a pulse frequency of 15 Hz, and a quiet time of 2 s was performed to record the amperometric responses for simultaneous detection of CEA and AFP.

### **Optimization of detection conditions**

The effect of pH of absorption solution was studied over the pH range of 4.0-6.5 (Fig. S5A). As shown in curve a, the maximum adsorption rate of the NGC hybrids for  $\text{Cu}^{2+}$  occurred at pH 5.0. Similarly, the adsorption rate of the NGC hybrids for  $\text{Pb}^{2+}$  as a function of pH of absorption solution was shown in curve b. It was indicated that the maximum adsorption rate was observed when pH was close to 6.0.

The immunoreaction time was a significant parameter for the capture and the specific recognition of the corresponding tracer on the NPS-PWE. With the increasing incubation time used in sandwich-type immunoassay, all the amperometric responses for CEA and AFP increased gradually and reached a plateau after 160 s (Fig. S5B), indicating a tendency to complete immunoreaction on the NPS-PWE surface. Thus, 160 s was used as the optimal immunoreaction time.

The effect of detection solution pH on the electrochemical signals of the  $\mu$ -OMEI was displayed in Fig. S5C. In the examined pH range, the maximum amperometric response of this  $\mu$ -OMEI occurred when pH was 4.5. Therefore, 0.1 M HAc/NaAc (pH 4.5) was selected as the detection solution.

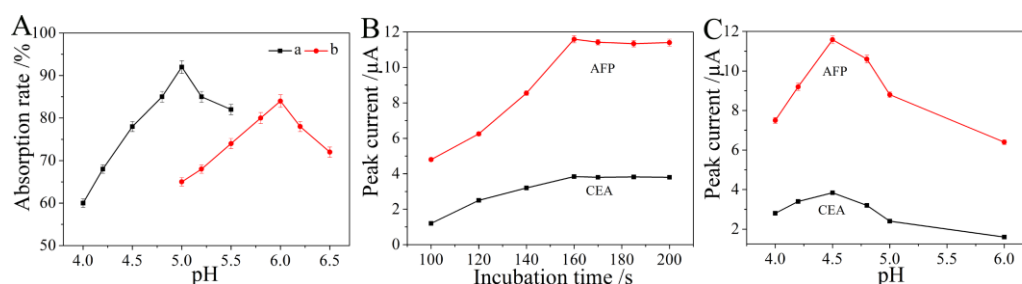


**Fig. S5** A) The effects of pH of absorption solution on the adsorption of (a) Cu<sup>2+</sup> and (b) Pb<sup>2+</sup>. Effect of B) incubation time and C) pH of detection solution for 0.1 ng·mL<sup>-1</sup> CEA and AFP, where n = 10 for each point.

### Analytical Performance

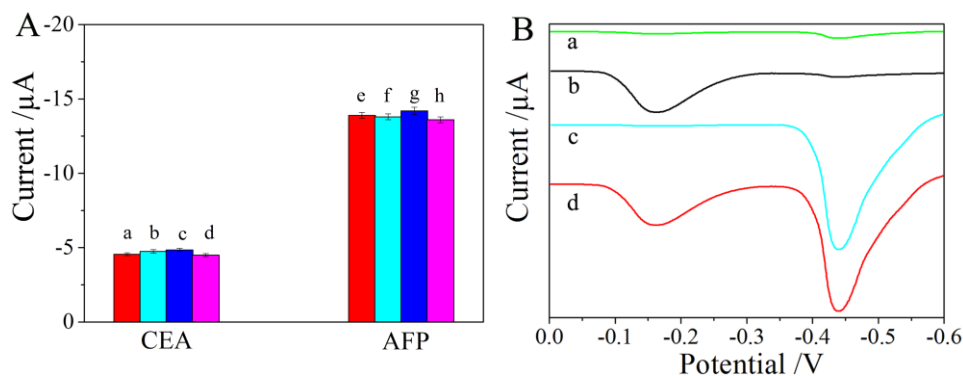


**Fig. S6** A) The specificity of the  $\mu$ -OMEI at the concentration of 1.0 ng·mL<sup>-1</sup> CEA and AFP with the interfere concentrations of (a, e) no interferes, (b, f) 100 ng·mL<sup>-1</sup> BSA, (c, g) 100 ng·mL<sup>-1</sup> hemoglobin, (d, h) 100 ng·mL<sup>-1</sup> glucose. B) Typical SWV immunoassay signals for the investigation of cross-reactivity: (a) 0 ng·mL<sup>-1</sup> CEA and AFP, (b) 1.0 ng·mL<sup>-1</sup> CEA solution, (c) 1.0 ng·mL<sup>-1</sup> AFP, (d) 1.0 ng·mL<sup>-1</sup> CEA and AFP in the sandwich immunoassay.

### Application in human serum samples

**Table S1** Assay results of human serum samples by the proposed and reference method

| Samples  | CEA concentration (ng·mL <sup>-1</sup> ) |                  |                    | AFP concentration (ng·mL <sup>-1</sup> ) |                  |                    |
|----------|--|------------------|--------------------|--|------------------|--------------------|
|          | Proposed method                          | Reference method | Relative error (%) | Proposed method                          | Reference method | Relative error (%) |
| Sample-1 | 21.2                                     | 21.8             | -2.8               | 10.2                                     | 9.88             | 3.2                |
| Sample-2 | 42.5                                     | 41.9             | 1.4                | 17.5                                     | 17.9             | -2.2               |
| Sample-3 | 54.7                                     | 53.6             | 2.1                | 53.5                                     | 52.7             | 1.5                |
| Sample-4 | 65.8                                     | 66.5             | -1.1               | 61.2                                     | 62.5             | -2.1               |
| Sample-5 | 72.3                                     | 70.6             | 2.4                | 85.7                                     | 88.4             | -3.0               |

**Table S2** Recovery of CEA in human serum samples

| sample | $c_{\text{CEA}}$<br>(ng·mL <sup>-1</sup> ) | added                   | detected                  | RSD<br>(%, n=10) | recovery<br>(%) |
|--------|--|-------------------------|---------------------------|------------------|-----------------|
| 1      | ×  | 0.1 pg·mL <sup>-1</sup> | 0.099 pg·mL <sup>-1</sup> | 3.1              | 99.0            |
| 2      | ×  | 20 pg·mL <sup>-1</sup>  | 20.04 pg·mL <sup>-1</sup> | 3.5              | 100.2           |
| 3      | ×  | 6 ng·mL <sup>-1</sup>   | 5.89 ng·mL <sup>-1</sup>  | 4.1              | 98.2            |
| 4      | ×  | 36 ng·mL <sup>-1</sup>  | 35.8 ng·mL <sup>-1</sup>  | 3.6              | 99.4            |
| 5      | ×  | 65 ng·mL <sup>-1</sup>  | 66.6 ng·mL <sup>-1</sup>  | 4.2              | 102.5           |
| 6      | ×  | 91 ng·mL <sup>-1</sup>  | 91.9 ng·mL <sup>-1</sup>  | 3.8              | 101.0           |

Each sample was repeated for ten times and averaged to obtain the recovery and RSD values.

Samples 1-6 were from healthy people; “x” represents not detectable.

## Reference

1. E. Carrilho, A. W. Martinez and G. M. Whitesides, *Anal. Chem.*, 2009, **81**, 7091.
2. X. Gong, X. Yi, K. Xiao, S. Li, R. Kodzius, J. Qin and W. Wen, *Lab Chip*, 2010, **10**, 2622.
3. J. X. Yan, L. Ge, X. R. Song, M. Yan, S. G. Ge and J. H. Yu, *Chem.–Eur. J.*, 2012, **18**, 4938.
4. R. Pelton, *TrAC Trends Anal. Chem.*, 2009, **28**, 925.
5. M. N. Kashid and L. K. Minsker, *Ind. Eng. Chem. Res.*, 2009, **48**, 6465.